

# Sodium Layer Monitoring at Calar Alto by LIDAR

David J. Butler<sup>a</sup>, Richard Davies<sup>a</sup>, Hayden Fews<sup>b</sup>, Micheal Redfern<sup>b</sup>, Nancy Ageorges<sup>b</sup>, Wolfgang Hackenberg<sup>c</sup>, Ralf-Rainer Rohloff<sup>d</sup>, Sebastian Rabien<sup>a</sup>, Thomas Ott<sup>a</sup>, Stefan Hippler<sup>d</sup>

<sup>a</sup>Max-Planck-Institut für Extraterrestrische Physik,  
Postfach 1603, D-85740 Garching, Germany

<sup>b</sup>Experimental Physics Department, National University of Ireland, Galway, Ireland.

<sup>c</sup>European Southern Observatory, Garching, Germany,

<sup>d</sup>Max-Planck-Institut für Astronomie, Königstuhl 17, D-69117 Heidelberg, Germany.

## ABSTRACT

Observations have shown the presence of sodium layer centroid height variations of a few hundred metres on timescales of tens of seconds<sup>1</sup>. As quality laser guide star (LGS) plus adaptive optics (AO) assisted astronomy, especially on large (8m+) telescopes, will require optimal scheduling of observations and regular laser and wavefront sensor focussing at sites where sporadic sodium layers are frequent, an ‘easy to use’ sodium layer monitor is required.

LIDAR offers a convenient means to achieve this. By pulsing the outgoing sodium laser and performing time-of-flight measurements on the returned photons we can acquire the altitude profile of the sodium layer. Unfortunately, conventional LIDAR requires the laser duty cycle to be very low, therefore large integration times are required. However, by using a cross-correlation technique the duty cycle can be increased to 50%, which gives far better performance. We present the details of this technique which involved amplitude modulation of the MPIA/MPE ALFA cw laser, as well as the following results of such LIDAR measurements performed in October 1999 at the 3.5m telescope at Calar Alto Observatory in Spain.

The altitude of the sodium layer at Calar Alto on 17<sup>th</sup> and 18<sup>th</sup> October 1999 was found to be at  $90 \pm 3\text{km}$  and there is evidence for sporadics on one of two nights with sporadic layer FWHM\* varying from  $\sim 240$  to  $350\text{m}$ . In addition, a noticeable layer FWHM change (excluding the sporadic layer) from  $\sim 13$  to  $\sim 5\text{-}7\text{km}$  was observed over the two nights. After flux and altitude calibration and correction of the projected altitude range, a very good agreement is found between sodium layer profiles derived from an auxiliary telescope and 3.5m telescope LIDAR observations. Using an intensity weighted centroid algorithm the centroid height of the sodium layer was observed to have a variation of  $< 500\text{m}$  in  $\sim 10$  minutes. Although, shorter timescale variations may be have been present, poor observing conditions and resulting reduced S/N prevents this analysis.

**Keywords:** laser guide star, LIDAR, sodium layer

## 1. INTRODUCTION

Great hopes are being placed in the current and future use of single and multiple sodium laser guide stars, for near IR image correction on medium to large (8m+) telescopes and beyond. A crucial element of the sodium laser guide system is the sodium layer.

The sodium laser guide star (LGS) relies on resonant backscattering of a laser tuned to the D<sub>2</sub> absorption line of naturally occurring sodium in the mesosphere. The intensity of the LGS produced depends on the laser launch power, polarization state, atmospheric transmission and the sodium column density. This must be sufficiently high for the associated AO system to correct high order wavefront aberrations. As the sodium layer has seasonal variations there may be some periods where the LGS is more effective. We would like to identify these times to enable more efficient scheduling of telescope time. However, the sodium layer also fluctuates on very short timescales. Sporadic layers occasionally appear which are thin (1-2 km) and dense, and cause altitude variations in the centroid height of the layer which can be incorrectly interpreted as a defocus term by the wavefront sensor (WFS). Although much work has been done to date at high and low latitudes sites, relatively little is known

---

Send correspondence to D.J.B.

E-mail: dbutler@mpe.mpg.de,

\*Full-Width at Half-Maximum

about the statistics of sporadic sodium layer occurrence (see O' Sullivan et al<sup>1</sup> 2000 and references therein) at mid-latitude sites like Calar Alto.

Statistically significant variations in the centroid height of the sodium layer on timescale of a few seconds or less, were not observed in previous sodium layer monitoring at Calar Alto<sup>1</sup>. Now, since we are interested in the properties of the sodium layer on timescales of tens of seconds to a few hours, an accurate, time efficient monitor of the sodium layer is required. Short timescale monitoring of the sodium layer centroid heights could facilitate automatic laser and initial WFS focusing, and derived statistics should allow optimal scheduling of laser guide star + adaptive optics assisted astronomy. Indeed, intervals of expected high sporadic activity could be avoided, if deemed necessary.

In October 1999, the ALFA (Adaptive Optics with a Laser for Astronomy) team comprised of MPIA and MPE teams in collaboration with NUI, Galway (Ireland) succeeded in installing a LIDAR system at the 3.5m telescope at Calar Alto Observatory in Spain. ALFA<sup>2</sup> is developed by MPIA and MPE and is run by CAHA (Centro Astronómico Hispano Alemán). One important feature of such a system is the ability to continue the process of obtaining long term statistics of short timescale variations of the properties of the sodium layer in a consistent and time efficient manner. In this paper, the experiment and the reasoning behind it is explained. We describe (a) the novel idea of amplitude modulation of the ALFA cw sodium line laser in order to launch a pseudo-random train of  $1\mu\text{s}$  laser pulses (b) the collection of returned photons in short (250ns) time bins and (c) reconstruction of the sodium layer profile by cross-correlating the returned sequence of photons with a modified representation of outgoing laser pulse sequence. In addition, we include our results of LIDAR observations of the sodium layer at Calar Alto during two nights in October 1999.

## 2. EXPERIMENTAL PROCEDURE

When using sodium fluorescence to measure the sodium density profile, it is important that we know the relation between them, which can depend on both the laser intensity and the sodium column density. If the laser intensity in the mesosphere is higher than  $6 \text{ W m}^{-2} \text{ MHz}^{-1}$  then saturation losses will reach 50%. Since this is caused by the finite decay time of excited sodium atoms, it depends only on the laser intensity. Additionally, the sodium column density is low enough ( $\sim 10^{13} \text{ m}^{-2}$ ) that very little of the laser power is absorbed (typically 4% at zenith, reaching a maximum of 10% at a zenith distance of  $60^\circ$ ), so the intensity does not change much through the layer, and saturation will affect the whole layer equally. The modulated beam of the ALFA laser (which has a 10 MHz bandwidth) has a peak power of around 2 W, so in the mesosphere the 1 arcsec spot will anyway not saturate the sodium. Thus we can be sure that the fluorescence and density profiles of the mesospheric sodium have a direct relation.

Although a classical LIDAR approach consisting of single, say  $1\mu\text{s}$  pulses, can allow the sodium layer profile to be constructed, this is prohibited in our application because (a) pulse separations  $> 70\mu\text{s}$  at zenith and  $> 140\mu\text{s}$  at a zenith distance of  $60^\circ$ , for example, are required to avoid overlapping of successive pulses in the sodium layer, thereby removing confusion over the location of photon emission and (b) the laser can only be modulated and not Q-switched. The resulting small mark/space ratio would greatly reduce the mean power and hence the effective signal to noise. This would require long integrations and would prevent monitoring of the sodium layer profile on timescales of tens of seconds, which is what we are primarily interested in. As a result we use a (known) pseudo-random sequence to modulate the laser pulses, with a total ‘On’ time of 50%. The pseudo-random sequence must be sufficiently long to exceed the maximum round-trip time under any circumstances. If  $S_0$  is the out-going laser pulse sequence then the returned stream of photons results from the convolution of  $S_0$  with the sodium profile  $N \otimes S_0$ . The intrinsic sodium abundance profile,  $N$ , can be recovered from the data by cross-correlating it with the original pulse sequence, because the auto-correlation of the sequence is very close to being a delta-function. Thus we find

$$S_0 \otimes (S_0 \otimes N) = N$$

We use a variation of this by over-sampling, so although the pulses are  $1\mu\text{s}$  long we collect the returned photons in  $0.25\mu\text{s}$  time bins. Now to recover the sodium profile we consider the emitted laser pulse sequence as a sequence of impulses,  $S_1$ , four times longer in which each digit of  $S_0$  is padded with zeros. If the profile of a pulse from the laser is denoted by  $L$  then we can consider the emitted sequence as  $S_1 \otimes L$ , and the returned flux is  $S_1 \otimes L \otimes N$ . We can calculate the following cross-correlation

$$S_1 \otimes (S_1 \otimes L \otimes N) = L \otimes N$$

which gives the convolution of the sodium profile with the pulse profile.

Finally, a correction has to be made to this profile to compensate for the height at which each photon was scattered because the telescope mirror subtends a smaller solid angle for emission that originates higher in the atmosphere.

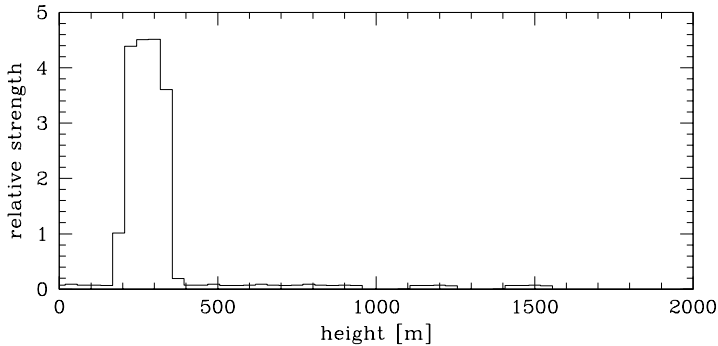


**Figure 1.** The profile of the  $1\mu\text{s}$  laser pulse, measured by scattering the beam from the telescope dome. The profile is close to being square-wave and has a FWHM of 150 m, as expected. The height offset of 270 m is due to a delay of  $1.8\mu\text{s}$  between the pulse generator, modulator, and detector. It has been subtracted from all subsequent height measurements.

The shape of the pulse profile, and any height offset which might arise due to timing delays, can be found by carrying out the procedure with the telescope dome closed: this provides a single scattering layer at almost zero distance. The cross-correlated data, shown in Fig. 1 shows that there is a height offset of 270m. This is equivalent to a delay in the system of  $1.8\mu\text{s}$ , and has simply been subtracted from all other derived heights. It can be seen that the laser pulse has a form close to a square-wave with a measured width of 150 m, which is what we would expect for a  $1\mu\text{s}$  pulse. For high signal-to-noise data, this profile can be used to deconvolve the sodium layer profile to yield a height resolution better than 100 m.

### 3. EXPERIMENTAL SET-UP

#### 3.1. The Laser

The ALFA-Laser system<sup>3</sup>, situated in the Coudé laboratory of the 3.5m telescope at Calar Alto Observatory in Spain, is used to provide a sodium reference star in the Earth's sodium layer at 90km altitude for high order adaptive optics correction. It typically has a V band magnitude of 9-10. The laser system consists of a 4W Argon-ion (Coherent model Innova 400) pumped cw dye-jet laser (Coherent model 899-21) tuned to sodium D<sub>2</sub> line (589nm) with a 10MHz bandwidth. The laser is circularly polarized, pre-expanded and then sent to the 50cm diameter laser launch telescope via a remotely controllable series of relay mirrors<sup>4</sup>. The launch beam has a 15cm diameter and is 2.9m away from the science telescope optical axis.

#### 3.2. Laser Modulation

As described in section 2, close to square wave amplitude modulation of the laser beam at MHz rates was desired to achieve the required height resolution and a maximum returned flux. An acousto-optical modulator (AOM) was used to produce the pulse pattern, also described in section 2, with the modulator driven by a pulse generator (HP 81101A).

Short ( $1\mu\text{s}$ ), square wave laser pulses would be ideal for the LIDAR experiment, since for any given pulse pattern, square wave geometry provides a maximum output signal and therefore provides data with a maximum S/N level (if not background limited). Indeed, it is the pulse rise (and fall) time that governs the squareness of a pulse and in the AOM the rise time is dependent on beam diameter. In order to achieve a pulse rise (and fall) time of  $<100\text{ns}$  the collimated ( $\sim 1\text{mrad}$ ) 1mm diameter sodium laser was passed through two lenses, each of focal length 250mm, and the modulator was centred about 1cm in front of the focus of the first lens. The optical power density was  $< 300\text{Wmm}^{-2}$ . As seen in figure 2, three flip and two folding mirrors (broad band, dielectric) were used to steer the beam from its nominal path. After the modulation optics, the beam is passed to the beam pre-expander and along the optical train to the launch telescope. An adjustable shutter placed between the lenses and after the modulator was used to block all spots except the chosen first order spot. Some second order light passed through to the beam expander but this was largely blocked by the beam stop aperture. The first order beam power was maximised by reducing the driver output power to close to the minimum, then finding the optimal Bragg angle of the incident laser on the crystal by monitoring an optical power meter, and finally by setting the driver output power that maximises the first order beam optical power.

Although we only achieved a modulated laser system efficiency of  $\sim 55\%$  from the laser laboratory to the launch telescope in our first experiments ( $\sim 80\%$  nominal, unmodulated laser), the hope is to improve on this for future LIDAR observations.

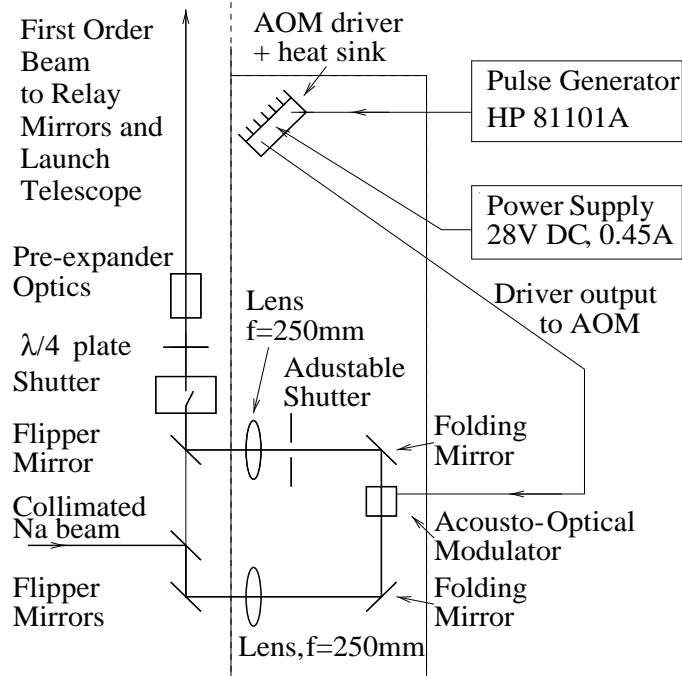


**Figure 2.** Laser Modulation Set-up in the Laser Laboratory. The optical train after the pre-expander has a shield.

Laser power was measured immediately prior to the launch telescope using a bolometer in the laser diagnostics box<sup>5</sup>. Given the pseudo-random modulation sequence, the average laser power was  $1.1\text{W} \pm 0.1$  at the end of the experiment on 17<sup>th</sup> Oct. 1999 and with launch telescope mirrors, each of reflectance  $\sim 0.8$ , an average of  $1.1\text{W} \times 0.8^2 \sim 0.7\text{W}$  exited the launch telescope.

#### 4. DATA COLLECTION

The data collection was composed of three parts: an Avalanche Photo-Diode (APD) set-up within ALFA (figure 3), the computer located in the telescope control room as well as laser star acquisition.

##### 4.1. Optical System

The accuracy of LIDAR data is limited by the timing resolution of the detector. For this reason CCD detectors are not suitable, and PMTs (photo-multiplier tubes) are more commonly used. However, PMTs have quite a low quantum efficiency (QE  $\sim 10\%$ ). This can be offset by adding several consecutive LIDAR frames together into one ‘exposure’, or alternatively increasing the laser launch power or using a larger collecting telescope. As we are interested in observing very short lived ‘sporadic’ structures in the sodium layer, a short exposure time is desirable. By using the cross-correlation approach described in section 2 we have increased the average launch power. Therefore improving the detector QE will directly increase the temporal structure observable in the mesosphere. To this end we used an actively quenched silicon Avalanche PhotoDiode (Perkin Elmer) with a QE  $> 70\%$ . Actively quenched APDs minimize the dead time after each detected photon to  $\sim 20\text{ns}$ . Statistical simulations show that we only expect 1-2 photons to be detected every micro-second under the brightest night conditions. Therefore, this dead time will not affect our measurements. The APDs have no readout noise associated with them and the dominant source of noise is not any APD dark counts ( $< 1000 \text{ s}^{-1}$ ), but background counts, including sky counts and stray light around the sodium line transmission filter in the optical path in ALFA. However, much more serious was the presence of IR LEDs inside the ALFA bench, on motor encoders for example. Although every effort was made to remove these the overall background count rate was  $\sim 7000\text{-}8000 \text{ counts s}^{-1}$ . This is not a problem, however, as the cross correlation is very good at rejecting background noise.

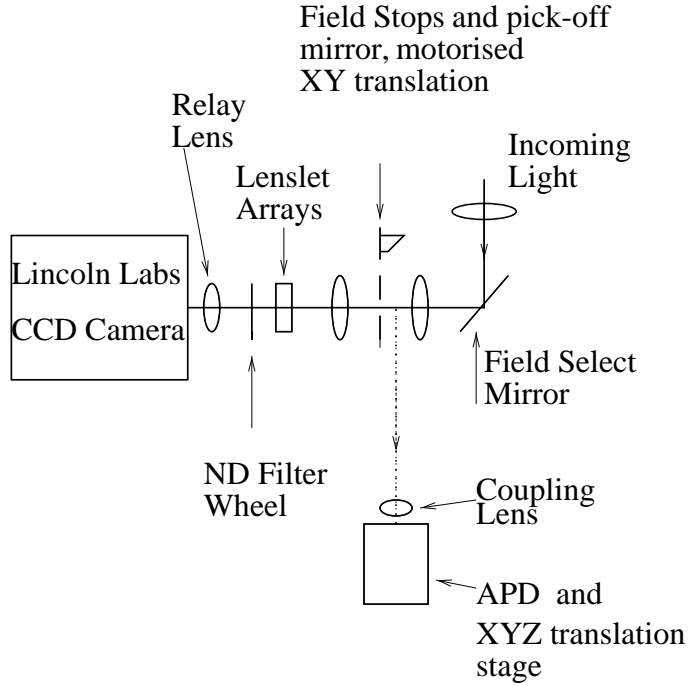


**Figure 3.** APD set-up at the Shack-Hartmann Sensor in ALFA.

In mounting the detector on the telescope we only had access to the F/25 focus, at which the plate scale was  $0.42\text{mm arcsec}^{-1}$ . Given a  $200\mu\text{m}$  diameter APD active area, the APD plate scale is  $\sim 0.03\text{mm arcsec}^{-1}$ . Since the LGS FWHM is typically  $< 3$  arcsec (1 arcsec seeing), the chosen APD field of view (FoV) of 6 arcsec is well matched, and in addition, as seen in the LIDAR results shown later in section 5, this FoV restricts data collection to photons from distances of  $90 \pm 30\text{km}$ . So, a  $\times 12$  magnification of the image of the APD on to the F/25 focus was required. In order to do this without losing any light requires a high numerical aperture lens ( $\text{NA} \sim 0.6$ ), placed very close to the front surface of the APD to ensure that working distances remain manageable. Alignment of the optical system was performed actively, using an illuminated white fibre source placed at the F/10 focus to simulate the laser guide star. The white light fibre was chosen instead of the laser reference fibre in order to maximize the count rate at the APD.

In order to pick off the sodium beam and send it to the APD, a 0.5 inch diameter dielectric pick-off mirror was placed at  $\sim 45^\circ$ , close to the F/25 LGS focal plane field stop stage, which is usually used to block Rayleigh scattered light and is remotely movable in two axes in the plane of the ALFA optical bench. The APD power supply was bolted to the ALFA bench. In addition to the usual dust and light shields surrounding the ALFA bench, heavy black cloth was attached to ALFA to block stray external optical light from reaching the APD.

#### 4.2. Data Acquisition

The APD module outputs a TTL pulse every time a photon is received. A similar TTL sync signal is produced from the signal generator at the start of every 16Kbit long pseudo-random sequence. These two signals are received by a Multichannel scaler (MCS) where timing information is recorded. The MCS card (Fastcomtec MCD-2) consists of 128k channels, each of which correspond to 250ns intervals. When the sync pulse is received the MCS starts at the first channel, and will increment its value if it receives a count from the APD within 250ns. After this time it moves to the next channel and again counts the number of pulses coming from the APD. This procedure continues until the next time a sync pulse is received, when the MCS starts from the first channel again. As each interval is 250ns long, and each laser pulse is  $1\mu\text{s}$ , returned flux is over-sampled by four so that there is sufficient timing resolution to satisfy Shannon's sampling criterium. The MCS is not perfect however, in that it has its own dead time between channels of 0.5ns. This is not significant for the APD channel as it only has the same effect as reducing the collection area of the telescope by 0.2%. Its effect can occasionally be seen in the sync channel, and this is why we have twice as many channels as should ever be needed. Occasionally the MCS will miss the sync pulse and the collected data will

'overflow' into these other channels. Although, this data is not useful, it prevents the rest from being corrupted. The system should be capable of producing a sodium profile with very good signal to noise every few seconds. Unfortunately, on the two nights available the observing conditions were so bad that photon return flux was much lower than expected. This in no way effects the accuracy of the measurement, but longer exposure times were required to give good S/N profiles.

For every integration, two files are created. One includes a record of the exposure epoch, integration time, data collection formats, data file name while the other one contains the counts in each of the time bins. About 0.26 MB was required for a 10s collection interval.

Since it is important that the telescope can move freely, electronic pulses from photons detected by the APD were sent via co-axial cable to a BNC plug board on the telescope which routes the signal from there to the control room where the data collection PC was located.

#### 4.3. Laser Star Acquisition

Since the APD is a single element device, a 2D detector is required for efficient laser spot acquisition. So, acquistion of the sodium laser on the APD consisted of two parts:

Firstly, prior to the observations, the APD was aligned with an arbitrary point on the WFS by picking off the white light reference beam and adjusting the APD stage so as to maximize the count rate on an APD event counter.

Secondly, at the beginning of the observations, the laser was acquired on the TV guider and steered with the field select mirror to the nominal position for coincidence with the WFS. Next, one of the white light fibre spots on the WFS was marked and afterwards the correponding sodium laser WFS spot was moved to this mark. Following this, the pick-off mirror was moved in and integration was started.

Although the observation plan was to consider the laser star at zenith, it was desirable to test the robustness of the system to flexure. So, the telescope was moved arbitrarily to about 15 degrees from zenith and the change in optimal pick-off mirror position was found to be negligible.

### 5. SODIUM PROFILES FROM LIDAR

The first measurements using this technique with ALFA were obtained on the nights of October 17<sup>th</sup> & 18<sup>th</sup> 1999 under extremely poor weather conditions. On the first night the seeing was 4 arcsec or more. Even though the laser is launched with a 15 cm beam, in such bad seeing this is much more than a few  $r_0$  and so the size of the LGS is affected. The final size of the LGS as seen from the ground is therefore at least 6arcsec. As a result, significant light was lost from the detector's FoV. On the second night there were thin cloud layers at 6 km and 9 km (observed by the LIDAR system from the light they scattered). Simultaneous observations of the LGS from a nearby telescope showed that the observed flux was reduced by a factor of 30 by these cloud layers. The only effect this has on LIDAR is to reduce the signal-to-noise and invalidate absolute flux calibration; the height and profile information (which arise solely from time-tagged data) are unaffected, and as such the first results, shown in Fig. 4 are very encouraging. These data have been convolved with a low-pass digital filter to give a smoothing of 500 m, and only the range encompassing the mesosphere plotted. Additionally, the total flux detected has been normalised for each night, a process which is not normally necessary but which we use in this case because of the significant flux variations due to clouds.

The Rayleigh cone, which is bright at altitudes less than  $\sim$ 20 km is not visible in any figure. This is not surprising because the 6arcsec FoV of the APD means that, since we launch the laser 2.9 m off-axis from the main telescope, we can only observe heights in the range  $90 \pm 30$  km. The reason we were able to observe cloud layers at  $< 10$  km is simply because there was so much scattered light from the defocussed image of the pupil on these layers, that we could detect it  $\sim 1$  arcmin away.

Due to the height adjustment made to the derived profile, the noise is also strongly dependent on height. It has been determined from a blank region in the profile, in the height range 10–60 km, which is as large as possible so that both the photon noise (including background) and the correlation noise are implicit in the estimate. The measurement is made after smoothing with the same filter as for the data in Fig. 4, but without having made the height adjustment because at this stage the noise is independent of height. The raw value can then be scaled to the required height in exactly the same way as for the data, the values quoted here being scaled to 90 km. It should be noted that the noise at 100 km is 25% more than, and at 80 km 20% less than, that at 90 km. The  $3\sigma$  level is shown using dashed lines in Fig. 4.

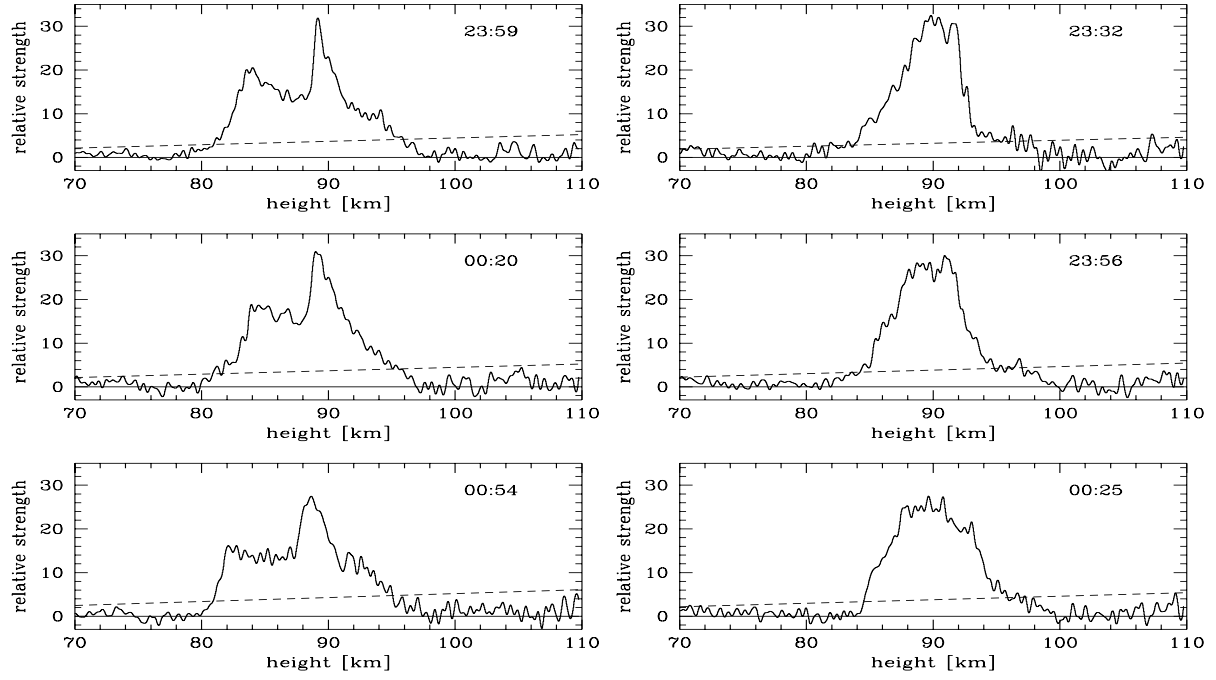


**Figure 4.** Profiles of the sodium layer taken at 3 different times on two consecutive nights: Oct 17<sup>th</sup> (left) and Oct 18<sup>th</sup> (right). The UT start time of each frame, each from 30 sec integrations, is shown. The  $3\sigma$  noise level (dependent on height) is shown as the dashed line; details of how it is determined are given in the text. Heights are given in km above Calar Alto Observatory which is itself at 2.2 km, and show that on these nights the sodium had a centroid height of 92 km above mean sea level. The difference in profile between the 2 nights is substantial.

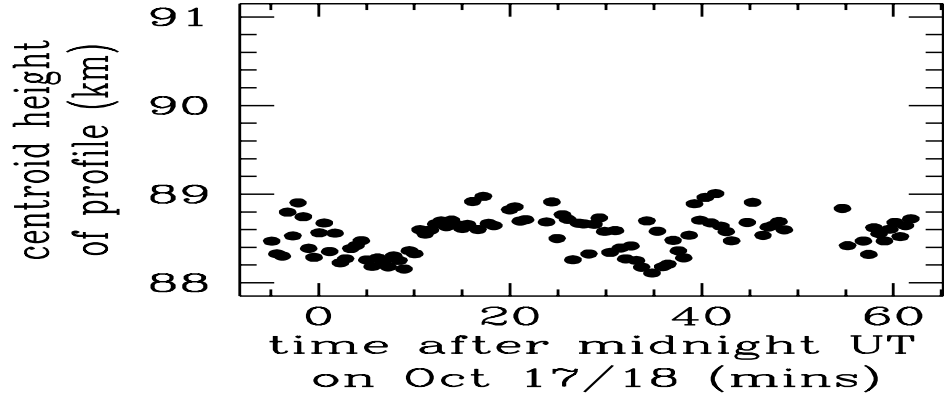


**Figure 5.** Plot of intensity weighted centroid height of sodium profile over time on 17/18 Oct. 1999. See text for additional details.

### 5.1. Results

The sodium layer above Calar Alto on 17<sup>th</sup> and 18<sup>th</sup> October 1999 was found to be at  $90 \pm 3$  km (Fig. 4). Evidence for sporadics on one of two nights was found with sporadic layer thickness varying from  $\sim 240$  to  $350$  m. In addition, it can be seen in Fig. 4 that a prominent change in layer FWHM (excluding the sporadic layer) from  $\sim 13$  to  $\sim 5$ - $7$  km was observed over the two nights.

This leads to a question about the effect of spot size variations in the WFS. We know that WFS sodium spot images

can become elongated depending on the position of the laser launch telescope relative to the science telescope pupil. Larger telescope mirrors subtend larger angles for a given sodium layer height and the outermost WFS subaperture images suffer the most elongation. This is not observed with ALFA due to the WFS pixel size of about 0.5 arcsec and is consistent with simulations<sup>6</sup>. The (LA<sup>3</sup>OS<sup>2</sup>) simulation code<sup>7</sup>, which considers a 3D sodium layer and propagation of light through a model atmosphere and astronomical AO system, was used to examine the effect of sodium layer FWHM changes on the spots seen in the Shack-Hartmann Sensor (SHS). This simulation indicates that while observing at zenith with the ALFA system, no significant change in the spot FWHM is expected in the cases of FWHM of 13km and 7km. However, the projected sodium layer structure is a function of zenith distance. Considering a zenith angle of 60° the observed FWHM would be 14km and 26km respectively and, in the case of a 26km layer, a FWHM change of about 0.3 arcsec could be expected in very good seeing conditions ( $r_o = 30\text{cm}$ ), with small WFS pixels (eg 0.2 arcsec pixel<sup>-1</sup>). With 0.5 arcsec pixel<sup>-1</sup>, no significant change is expected to be seen with ALFA in median seeing of about 1.2 arcsec.

Although, it can be seen that the amplitude of the sporadic layer is about two times that of the underlying sodium profile, similar to the factor of 2-3 observed during the September 1997 observations<sup>1</sup>, it provides only a lower bound because data smoothing was employed. A georges et al<sup>8</sup> (2000) provides a summary of the sodium layer monitoring observations made at Calar Alto during 1997-1999.

Using an intensity weighted centroid algorithm the centroid height of the sodium layer was observed to have a variation of < 500m in ~ 10 minutes (Fig. 5). Although, shorter timescale variations may have been present, poor observing conditions and reduced S/N prevents this analysis. To appreciate the implications of centroid height changes, consider that such changes, if uncorrected, can exceed the wavefront phase error budget of instruments like VLT/NAOS. Here, a centroid change of ~ 230m can produce defocus rms phase errors of ~ 37 nm rms, greater than the error budget of 15nm rms<sup>9</sup>.

## 6. DIRECT IMAGING

### 6.1. Observations from an auxiliary telescope

In order to independently validate the LIDAR observations, the sodium star was imaged from a 2.2m telescope 260m away on a nearly pure North-South axis. A 2048×2048 pixels SITE#1d CCD camera was installed at the Cassegrain focus of this telescope, with a 0.53 arcsec pixel scale. A narrow band interference sodium filter was used.

During the 5 allocated nights, the laser could be launched on only 2 consecutive nights, due to bad weather conditions. On these two nights, a profile of the sodium spot could be acquired simultaneously with the LIDAR experiment at the 3.5m telescope. This section concentrates on the comparison of the data.

To achieve a meaningful comparison of the sodium layer profiles from the LIDAR and 2.2m imaging data, the latter was acquired within 30s of the LIDAR data. Each consisted of 30s exposures, tagged with the UT start time from the computers in the respective telescopes.

Since no sky frames were acquired at the 2.2m, no sky subtraction was applied to the imaging data. Only a dark of equivalent integration time was subtracted before flat-fielding with a dome flat. Bad pixel correction has also been applied. In a cosmetic final phase, star trails crossing the sodium plume or Rayleigh beam have been removed by thresholding the data. Fig. 6 illustrates a typical result.

### 6.2. Altitude and Flux Calibration

Each projected sodium profile was obtained by taking a cut through an elongated LGS image followed by flux and altitude calibration so that it could be compared with the corresponding LIDAR sodium layer profile.

To increase the signal to noise of the sodium profile derived from CCD imaging, pixel values over the 10 pixels perpendicular to the altitude axis were co-added. Due to telescope separation and the alignment of altitude with the CCD frame rows, the altitude at each point,  $x$ , in the projected profile can be determined using:

$$\text{altitude} = z_0 + (d * \tan(\alpha - (x_0 - x) * \text{pixscale})), \quad (1)$$

where  $z_0$  is the altitude of the observing site (2.2km),  $d$  the distance between the telescopes,  $\alpha$  the elevation of the auxiliary telescope and  $\text{pixscale}$  is the pixel scale of the camera used.  $x_0$  has been chosen as the middle of the CCD FoV. Using this formula, we noticed a difference in altitude, and altitude range between the imaging and LIDAR data. To obtain a similar altitude range for both sets of data, the 2.2m elevation had to be considered 7.12 arcmin higher than what was indicated at the

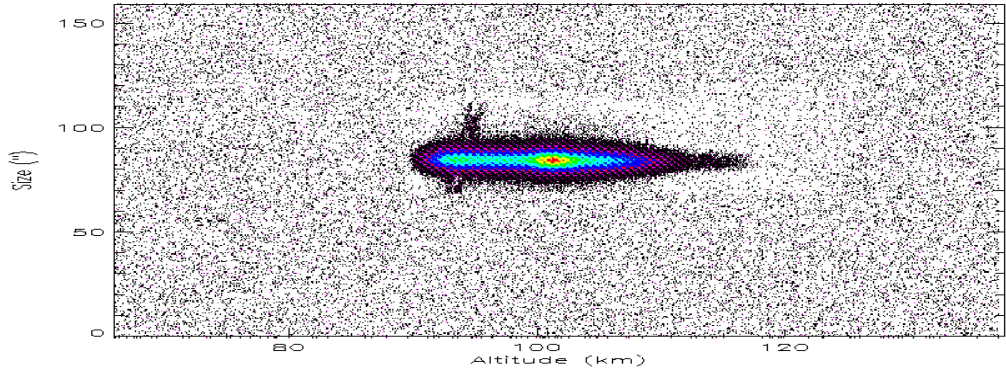


**Figure 6.** Typical image of the ALFA laser, as observed from the 2.2m telescope situated 260m away. This image is an extract from the full size image observed, and it has been cleaned of star trails, except for the one seen on the left of the sodium plume.

telescope. The elevation offset may be attributed in part to the fact that the laser may not have been pointing exactly at zenith as well as to possible pointing errors at the 2.2m telescope, something which is consistent with a repeated offset of calibration stars from the CCD frame centres. but here as well this could be due to poor stellar coordinates. As a result, no definitive answer can be given why, to match the altitude of the LIDAR data, the elevation of the 2.2m telescope had to be raised by 7.12 arcmin.

Once the data was calibrated in altitude, a flux calibration was applied: the integrated flux, of the 2.2m data, between 70 and 110km, was forced to equal the integrated flux (in the same range) of the LIDAR data.

### 6.3. Comparison with LIDAR data

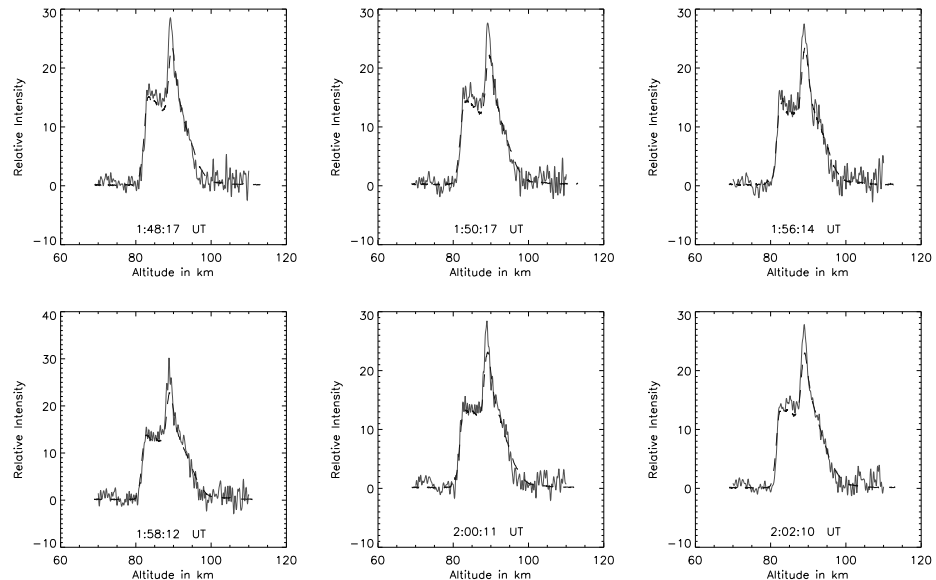


**Figure 7.** Results of LIDAR experiment results from Oct. 17<sup>th</sup> are compared with the sodium profile derived from the 2.2m telescope observations (dashed line). See the text for further comments.

A very good agreement can be found between the data obtained with two different observing techniques (Fig. 7). Imaging of the sodium layer gave profiles with better signal to noise than the LIDAR technique but this can be explained by a reduced count rate in the FoV due to poor seeing.

Here, observations have only been done with the laser pointed at zenith. Any other elevation of the laser launch could have been used, but more careful altitude calibration would have been required. We conclude that the LIDAR system is more useful than the imaging technique because (a) a suitable telescope for imaging would be required which is not practical at an astronomical observatory and (b) the height of the sodium layer is readily and more accurately determined with the LIDAR based approach.

Accounting for noise differences, the amplitudes of the sporadic layer profiles within each panel, as well as differences in the underlying intensity profiles are seen to differ slightly. This is because two different observing techniques are compared; LIDAR was used with a height resolution of about 150m, coupled with additional amplitude reduction due to smoothing of the data, and direct imaging of the projected sodium layer.

## 7. FUTURE

Continued sodium layer monitoring at Calar Alto is planned. The aim is to accumulate long term statistics of sodium abundance variations and the frequency of occurrence of sporadic layers. It will also be interesting to exploit LIDAR as a potentially very important tool for both time efficient and accurate focusing of the laser and the WFS.

Centroid height changes of a few hundred metres are expected to have important implications for LGS AO image correction on 8m+ telescopes, especially blueward of H band. Extrapolating from experiences with ALFA-LIDAR, simultaneous science observing and LIDAR observations may be an option if more than 4W cw sodium laser power can be achieved. Assuming 4W of laser power, which allows excellent high order ALFA image correction given 1 arcsec seeing or better and good atmospheric transparency, we can derive from the October 1999 observations where the laser was on 50% of the time that  $\leq$  8W laser power would be required if there is  $\geq$  50% laser amplitude modulation ‘On’ time. Feedback of centroid height changes to a calibrated laser star focus algorithm would allow minimum laser spot size to be maintained and in addition calibrated initial WFS focusing would be facilitated. Such a system is expected to be of importance for observing facilities like the VLT.

## ACKNOWLEDGMENTS

Jesus Aceituno and Robert Weiss are thanked for valuable assistance during the experiment set-up. Karl (Sam) Wagner is thanked for his electronics related assistance. Élise Viard’s help with the (LA<sup>3</sup>OS<sup>2</sup>) simulation code is very much appreciated. DB, RD, HF and NA acknowledge funding from the TMR European Network for Laser Guide Stars at 8m Class Telescopes under contract ERBFMRXCT 960094.

## 8. REFERENCES

- <sup>1</sup> C. M. M., O’ Sullivan, R. M. Redfern, N. Ageorges, H-C Holstenberg, W. Hackenberg, T. Ott, Rabien S., Davies R., Eckart A., “Short Timescale variability of the mesospheric sodium layer”, Experimental Astronomy, 2000, in press
- <sup>2</sup> S. Hippler,A. Glindemann,M. Kasper and P. Kalas and R. R. Rohloff and K. Wagner and D. Looze,“ALFA: The MPIA/MPE adaptive optics with a laser for astronomy project ”, Proc. SPIE, in Adaptive Optical System Technologies, 3353, Paper 05, 1998
- <sup>3</sup> A. Quirrenbach, W. Hackenberg, H.C. Holstenberg, and N. Wilnhammer, “The ALFA Dye Laser System ”, in: Laser Technology for Laser Guide Star Adaptive Optics Astronomy, Ed. N. Hubin, Garching, Germany, 1997, pp. 126-131, European Southern Observatory
- <sup>4</sup> Ott T., Hackenberg W., Rabien S., Eckart A., Hippler S., “The ALFA Laser: Beam Relay and Control System ”, Experimental Astronomy, 2000, in press
- <sup>5</sup> S. Rabien, T. Ott, W. Hackenberg, A. Eckart, R. Davies, M. Kasper, A. Quirrenbach, “The ALFA Laser and Analysis Tools ”, Experimental Astronomy, 2000, in press
- <sup>6</sup> Viard É., Delplancke F., Hubin N., Ageorges N., “LGS Na-spot elongation and Rayleigh scattering effects on Shack-Hartmann wavefront sensor performances”, SPIE, p8, 1999
- <sup>7</sup> M. Carbillet, B. Femenia, F. Delplancke, S. Eposito, L. Fini, A. Riccardi, É. Viard, N. Hubin, F. Rigaut, “LA<sup>3</sup>OS<sup>2</sup>: A Software Package for Laser Guide Star Adaptive Optics Systems”, SPIE, p378, 1999
- <sup>8</sup> N. Ageorges, N. N. Hubin, F. Delplancke & C. O’Sullivan, “Laser guide star: monitoring and light pollution ”, SPIE, Paper 4007-32, 2000
- <sup>9</sup> N. Ageorges, N. Hubin, R. M. Redfern, “Atmospheric Sodium Column Density Monitoring ”, in: ESO/OSA Topical Meeting on Astronomy with Adaptive Optics. Present Results and Future Programs, p3, 1999